Segmental and local dynamics of stacked thin films of poly(methyl methacrylate)

Tatsuhiko Hayashi and Koji Fukao*

Department of Physics, Ritsumeikan University, Noji-Higashi 1-1-1, Kusatsu, 525-8577 Japan

(Received 11 December 2013; published 13 February 2014)

The glass transition temperature and the dynamics of the α and β processes have been investigated using differential scanning calorimetry and dielectric relaxation spectroscopy during successive annealing processes above the glass transition temperature for stacked thin films of poly(methyl methacrylate) (PMMA) of various thicknesses. The glass transition temperature and the dynamics of the α process (segmental motion) of as-stacked PMMA thin films exhibit thin-film-like behavior, insofar as the glass transition temperature is depressed and the dynamics of the α process are faster than those of the bulk system. Annealing at high temperature causes the glass transition temperature to increase from the reduced value and causes the dynamics of the α process to become slower approaching those of the bulk. Contrary to the segmental motion, the relaxation time of the β process (local motion) of the stacked PMMA thin films is almost equal to that of the bulk PMMA and is unaffected by the annealing process. However, the relaxation strengths of both the α process and β process show a strong correlation between each other. The sum of the relaxation strengths remains almost unchanged, while the individual relaxation strengths change during the annealing process. The fragility index of the stacked PMMA thin films increases with annealing, which suggests that the glassy state of the stacked thin films changes from strong to fragile.

DOI: 10.1103/PhysRevE.89.022602 PACS number(s): 61.41.+e, 71.55.Jv, 81.05.Lg, 77.22.Ch

I. INTRODUCTION

Amorphous materials exhibit glass transition if the material is cooled from a high temperature to a lower temperature under an appropriate cooling condition. The physical mechanism of glass transition has long been investigated by many researchers [1]. However, the mechanism is still under debate. One of the most important key words for understanding the mechanism of glass transition is dynamical heterogeneity [2,3]. Recent experiments and simulations [4–6] clearly show the existence of dynamical heterogeneity, where the molecular motion related to glass transition shows cooperative behavior with respect to spacial correlation in the dynamics. The existence of dynamical heterogeneity can be directly related to the characteristic length scale which governs the mechanism of glass transition [7].

For the purpose of studying the characteristic length scale experimentally, the glass transition and related dynamics of thin polymer films have been intensively investigated by various experimental techniques. It has been reported that the glass transition behavior of thin polymer films shows a large deviation from that of the bulk [8,9], with few exceptions [10,11]. From investigations of glass transition in thin polymer films together with those near surface regions [12–17], it can be elucidated that there are mobile surface and/or interfacial regions which play a crucial role, especially in determining the glass transition dynamics in thin film geometry. Furthermore, it has recently been reported that ultrastable glass and liquids with enhanced orientational order can be obtained from the vapor phase using enhanced surface mobility [18–20]. Hence, an understanding of the role of the mobile surface and/or interface in the reorganization of the overall molecular structure and dynamics is now highly desired.

In stacked films of many thin polymeric layers, each layer with a thickness of several tens of nanometers, it is expected that the interfacial interaction between the thin polymer layers is much more enhanced when compared to the bulk system. Hence, the stacked thin polymer film can be regarded as an ideal system, in which the effect of interfacial interaction on the dynamics of molecular motion of the polymer films can be investigated, and the effect might also be controlled through an appropriate annealing above the glass transition temperature, T_g [21,22]. From such investigations, the crucial role of the interfacial interactions in determining T_g has been elucidated.

In our previous studies [23–25], the T_g and the dynamics of the α process of stacked thin films consisting of ultrathin layers of polystyrene (PS) or poly(2-chlorostyrene) (P2CS) have been investigated using differential scanning calorimetry (DSC) and dielectric relaxation spectroscopy (DRS) during the isothermal annealing process above T_g. Our measurements showed that the T_g of the as-stacked P2CS thin films is depressed and the dynamics of the α process are faster than those of the bulk system, similar to the single thin polymer films [26–28]. This result suggests that the interfacial interaction between thin layers plays a crucial role in the depression in T_g in thin film geometry. Furthermore, annealing above T_g increases the T_g of the stacked P2CS thin films up to the T_g of the bulk system.

In complex polymeric systems there are several dynamical modes in addition to the α process, which is related to the segmental motion of polymer chains. In poly(methyl methacrylate) (PMMA), the β process is observed in a frequency-temperature region separated from that of the α process. The dynamics of PMMA have been investigated using various experimental techniques, such as nuclear magnetic resonance [29], dynamics light scattering [30], and DRS [31–35]. On the basis of the experimental evidence, the molecular origin of the β process is thought to be due to the hindered rotation of the -$COOCH_3$ group about the C-C bond attached to the main chain, but including an intermolecular cooperativity. Here we question whether different dynamical modes are affected by

*Corresponding author: fukao.koji@gmail.com

 ©2014 American Physical Society

the interfacial interaction in similar or different ways. It has been reported from measurements using a photobleaching technique that PMMA has a mobile surface layer of 4 nm thickness at the bulk T_g [36,37]. Hence, it is expected that the as-stacked PMMA thin films will keep a mobile interfacial region and have a thin-film-like glass transition behavior, as observed in stacked PS or P2CS thin films [24].

In this study, the T_g and the dynamics of stacked PMMA thin films during the annealing process have been investigated using DSC and DRS in order to elucidate how the interfacial interaction affects the glass transition temperature and the dynamics of segmental and local motions. After giving the experimental details in Sec. II, the thermal properties of stacked PMMA thin films observed by DSC will be given in Sec. III, and the dynamics of stacked PMMA thin films revealed by DRS will be discussed in Sec. IV. Finally, in Sec. V, some conclusions and remarks will be made in order to compare the results of the present work with those of previous ones.

II. EXPERIMENTAL METHODS

A. Sample preparation

The PMMA used in this study was purchased from General Science Co. The weight-averaged molecular weight is $M_w = 5.4\times10^5$. Stacked thin films were prepared as follows [24]: single ultrathin films of various thicknesses were prepared on a glass substrate by spin coating from a toluene solution. The thickness of a single thin layer, d, was controlled by changing the concentration of the solution and evaluated from direct measurements by atomic force microscopy [27,38]. The film was floated onto the surface of water and transferred onto the top of the substrate or previously stacked thin films of polymers on the substrate. This procedure using ultrathin films of the same thickness is repeated until the total number of stacked thin layers reaches tens to several hundreds, as listed in Tables I and II. For the dielectric measurements, the first layer of PMMA is prepared directly onto the gold-deposited glass substrate, and the succeeding thin layers are prepared according to the above mentioned procedure. Gold is then vacuum-evaporated again to serve as the upper electrode. For the DSC measurements, a Teflon plate is used as the substrate. The stacked thin films consisting of several hundred thin layers are detached from the Teflon plate using a razor.

TABLE I. Samples prepared for DSC measurements: The thickness of the single layer d (nm), the number of stacked layers, and the lower and upper limiting temperatures of the glass transition region $T_{g,l}$ and $T_{g,h}$, the glass transition temperature T_g determined from the DSC measurements of stacked PMMA thin films.

d (nm)	No. of layers	$T_{g,l}$(K)	$T_{g,h}$(K)	T_g(K)
Bulk	1	377	395	389.6
80	60	373	392	386.7
48	100	372	389	384.0
15	300	370	388	380.8

TABLE II. Samples prepared for DRS measurements: The thickness of the single layer d, the number of stacked layers, and the temperature where the dielectric loss shows a peak due to the α process, T_α, at 100 Hz for as-stacked films (at $t_a = 0$ h).

d (nm)	No. of layers	T_α(K) (100 Hz)
65	10	402.8
41	30	401.5
15	50	399.5

B. DSC measurements

A commercial instrument, Q200 (TA Instruments), was used for DSC measurements. First, the DSC measurements on as-stacked PMMA thin films were done over a heating process from 303 to 420 K at the rate of 10 K/min and then for the subsequent cooling process down to 303 K at the same rate. These measurements were repeated three times in order to assess the reproducibility of the measurements. Following that, the stacked samples used for the measurements were annealed at 453 K for 12 h *in vacuo*. The same DSC measurements were then carried out for the heating and cooling processes between 303 and 420 K. A nitrogen gas flow of 30 ml/min was maintained during the DSC measurements.

C. DRS measurements

An LCR meter (Agilent Technology, 4284A) was used for dielectric measurements. The stacked samples for DRS measurements were prepared as shown in Table II. The temperature of the samples were then changed according to the program in Fig. 1. Before taking any dielectric measurements, the temperature of the as-stacked PMMA thin films was changed between 273 and 350 K (or 380 K) at the rate of 1 K/min in order to stabilize the samples for the dielectric measurements. The following temperature cycle was then repeated many times. One temperature cycle consists of two successive parts:

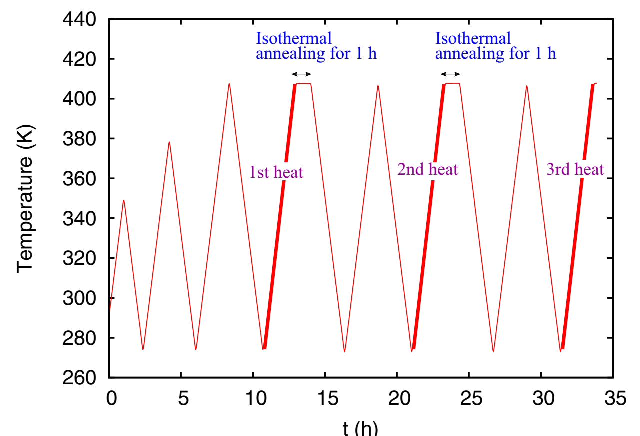

FIG. 1. (Color online) Temperature cycle assigned to stacked PMMA thin films for DRS measurements. The dielectric data measured during the heating process labeled 1st heat, 2nd heat, and so on are used for further analysis in this paper.

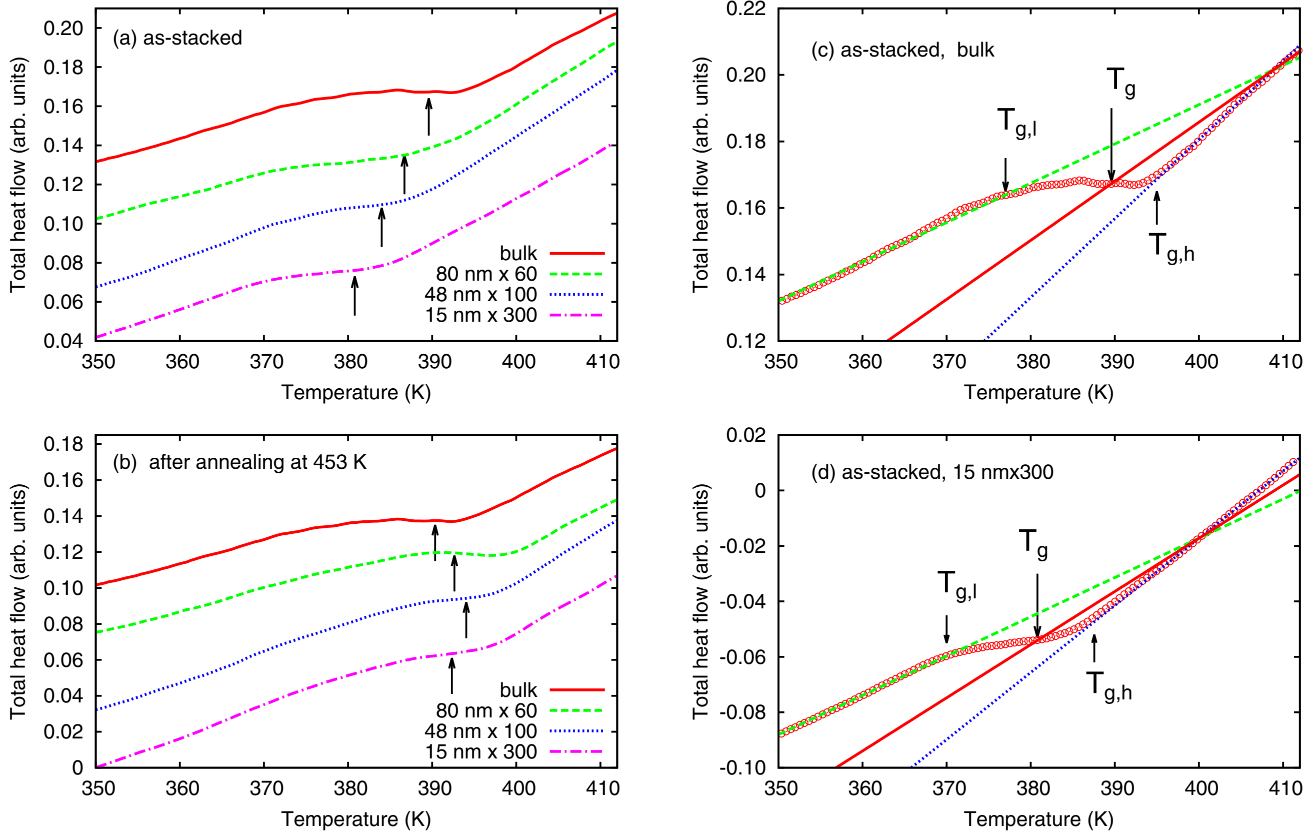

FIG. 2. (Color online) (a) Temperature dependence of the total heat flow observed by DSC measurements during the heating process for as-stacked thin films consisting of PMMA layers of 80, 48, and 15 nm thickness and bulk PMMA films. The arrows show the glass transition temperatures, which are listed in Table I. (b) Temperature dependence of the total heat flow observed in the same manner as in (a) for the same stacked PMMA thin films and bulk PMMA films after annealing at 453 K for 12 h. (c) and (d) Temperature dependence of the total heat flow for bulk PMMA films (c) and as-stacked thin films consisting of PMMA layers of 15 nm thickness (d). The green dashed and blue dotted lines are obtained by fitting of the data below and above the anomoluos glass transition regions. The red solid line is drawn so that the red solid line can go through the crossing point between the green dashed and blue dotted lines and the slope can be equal to the average value of the slopes between the two lines. $T_{g,l}$ and $T_{g,h}$ stand for the lower and upper limits of the glass transition region, respectively.

(1) Cooling and heating processes between 409 and 273 K at the rate of 1 K/min, carried out twice.

(2) After the ramping process, the temperature is kept at 409 K for 1 h (isothermal annealing at $T_a = 409$ K).

Throughout all the temperature cycles, dielectric measurements for the frequency range from 1 MHz to 20 Hz are repeated. One frequency scan takes about 50 s. Two of the same heat and cool processes are inserted between two isothermal annealing processes to check whether there is no significant change between the two serial heat and cool processes. As the thermal change in stacked PMMA thin films during the ramping process between 273 and 409 K can be much smaller than that during the isothermal annealing process (except for the first ramping process), the total time for which the sample is kept at 409 K can be regarded as the effective annealing time t_a in the present measurements.

III. THERMAL PROPERTIES OF STACKED PMMA THIN FILMS DETERMINED BY DSC

Figure 2 shows the temperature dependence of the total heat flow observed during the heating process at the rate of 10 K/min, for the stacked PMMA films consisting of thin layers of various thicknesses, as shown in Table I. In Fig. 2(a) there is a temperature region where the total heat flow shows anomalous temperature dependence. The averaged location of the anomalous signal can be regarded as T_g and is determined by DSC. Here the value of T_g is determined from the observed temperature dependence of the total heat flow as follows. First, two straight lines are determined by data fitting for the temperature ranges below and above the anomalous glass transition region, respectively, so that the observed data over the two temperature regions can be well reproduced by two different straight lines, as shown by dashed and dotted lines in Figs. 2(c) and 2(d). From these two straight lines, the third straight line [solid line in Figs. 2(c) and 2(d)] is produced so that the third line can go through the crossing point of the first and second straight lines and its slope can be equal to the average value of the slopes between the first and second lines. The value of T_g is determined as the temperature at which the third straight line obtained in the above intersects the observed curve of the total heat flow. The T_g obtained in this manner is 381 K for the as-stacked PMMA thin films consisting of 15 nm thick layers. Because the T_g of the bulk sample is 390 K, the T_g of the as-stacked PMMA thin films of 15 nm layer thickness is depressed by about 9 K from

the bulk value. Table I shows that the values of T_g for the as-stacked PMMA thin films of $d = 48$ nm and 80 nm are 384 K and 387 K, respectively. Hence, the T_g of the as-stacked PMMA thin films decreases from the bulk T_g with decreasing thickness of the single layer in the stacked PMMA thin films. Keddie *et al.* showed that the T_g of PMMA thin films supported on a gold-deposited substrate decreases with decreasing film thickness [39]. On the basis of these experimental results, it can be concluded that the glass transition of the as-stacked PMMA thin films has a thin-film-like character. Furthermore, the lower and upper limiting temperatures of the anomalous glass transition region, $T_{g,l}$ and $T_{g,h}$, are also given in Table I, to show the extent of the anomalous glass transition region.

Figure 2(b) shows the temperature dependence of the total heat flow observed for stacked PMMA thin films after annealing at 453 K for 12 h. In Fig. 2(b), the T_g for the stacked PMMA thin films is clearly shifted to the higher temperature side after annealing and converges with the value of the bulk system, although there is a scatter in the measured T_g values. It is expected that annealing at a high temperature above T_g could lead to a reduction and an eventual disappearance in the density gap at the interfaces between the thin layers stacked onto each other. Therefore, the decrease in T_g of the as-stacked PMMA thin films is strongly associated with the existence of the interfaces between the stacked thin layers. It should be noted that the observed results for the stacked PMMA thin films in this study are consistent with our previous experimental results observed for the stacked PS or P2CS thin films [24].

IV. DYNAMICS OF STACKED PMMA THIN FILMS DETERMINED BY DRS

As shown in Sec. III, the as-stacked PMMA thin films show a thin-film-like glass transition behavior, which changes to the bulk-like glass transition behavior by annealing above T_g. In Sec. IV experimental results observed by DRS for the stacked PMMA thin films during the annealing process are shown in order to elucidate the temporal changes in the molecular dynamics of PMMA chains in stacked thin films.

A. Temperature dispersion of dielectric loss spectra

Figure 3 shows the temperature dependence of the dielectric loss at 100 Hz for the stacked PMMA thin films consisting of 65-nm-thick layers during the annealing process at 409 K. In Fig. 3 there are two dielectric loss processes; one is the α process located around 400 K, and the other is the β process located at 333 K. The microscopic origin of the α process is segmental motion, and that of the β process is local motion, or the motion of the side branch attached to the PMMA main chain, as mentioned in Sec. I. In Fig. 3, the arrows show that the dielectric behavior of both processes changes with increasing effective annealing time t_a during the annealing process.

In order to evaluate the t_a dependence of the dielectric behavior of the α and β processes in greater detail, we evaluate several physical quantities such as peak temperatures, peak widths, and relaxation strengths of the two processes from the observed dielectric loss in the temperature domain. For this purpose, it is assumed that the temperature dependence of the dielectric loss spectra in a temperature domain at a given

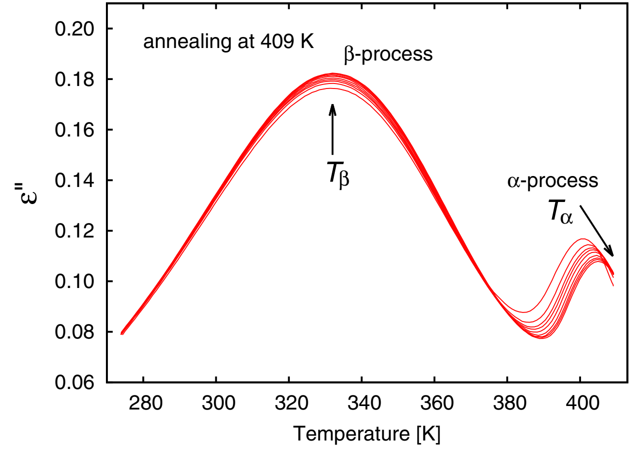

FIG. 3. (Color online) Dielectric loss spectra in the temperature domain at 100 Hz for stacked thin films of 10 PMMA layers of 65 nm thickness, observed during the annealing process at 409 K for $t_a = 0$, 1, 2, 3, 5, 9, 13, 17, and 21 h.

frequency can be described by the following formula:

$$\varepsilon''(\omega,T) = \sum_{i=\alpha,\beta} \frac{\Delta\varepsilon_i}{1 + ((T - T_i)/\Delta T_i)^2}, \tag{1}$$

where i is α or β, $\Delta\varepsilon_i$ is the relaxation strength of the i process, T_i is the temperature at which the dielectric loss shows a peak due to the i process, and ΔT_i is the width of the i process. Here it should be noted that the shape of the β process shows a small deviation from a symmetrical shape in the temperature domain, as shown in Fig. 3, although it is difficult to judge the symmetry of the α process. In order to take into account the asymmetry of the β process, we assume that ΔT_β is given by

$$\Delta T_\beta = \begin{cases} \Delta T_\beta^l & : \quad T < T_\beta \\ \Delta T_\beta^r & : \quad T > T_\beta, \end{cases} \tag{2}$$

while ΔT_α has the same value both above and below T_α.

B. T_α and T_β as a function of t_a

Figure 4 shows the dependence on annealing time of the peak temperatures, (a) T_α and (b) T_β, at various frequencies from 20 to 800 Hz during the annealing process at 409 K, for the stacked PMMA thin films consisting of 65-nm-thick layers. In Fig. 4(a), T_α increases monotonically from 400.6 to 404.1 K with increasing t_a from 0 to 24 h at 20 Hz. As the frequency increases from 20 to 800 Hz, the absolute value of T_α increases, but the T_α has a similar t_a dependence. On the other hand, in Fig. 4(b), the peak temperature T_β due to the β process shows almost no change during the annealing process and remains constant at a fixed frequency. Hence, we can say that the t_a dependence of the β process is distinctly different from that of the α process. As the frequency increases, the absolute value of T_β also increases at a given value of t_a. The temperature and frequency dependence of T_α and T_β of the two processes will be discussed in Sec. IV D.

In order to investigate the universal behavior of the change observed during the annealing process, it is assumed that the t_a dependence of T_α is given by the following simple exponential

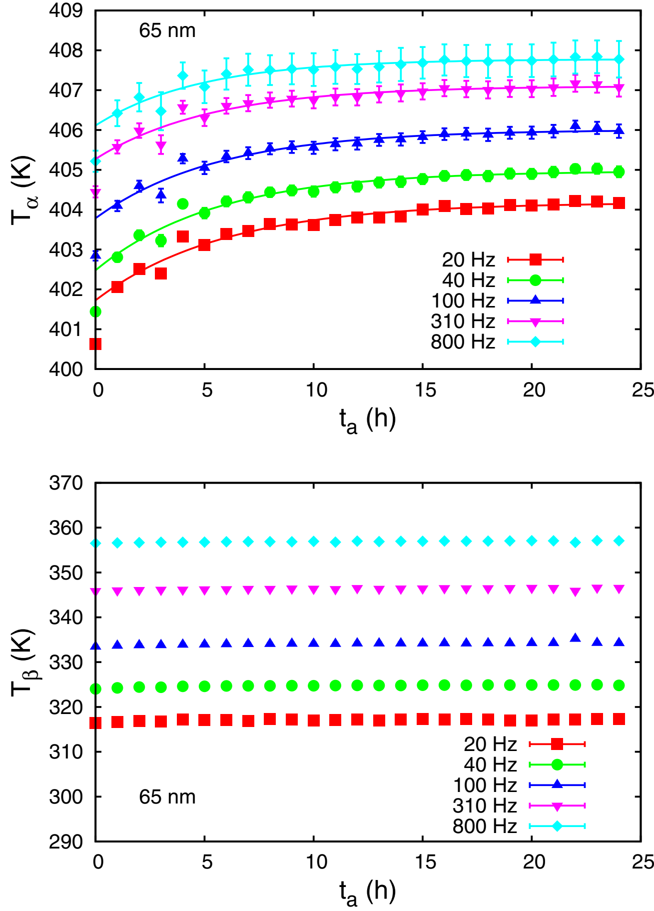

FIG. 4. (Color online) The dependence on annealing time t_a of the peak temperatures T_α and T_β at which the dielectric loss shows a peak due to the α and β processes, respectively, at various frequencies from 20 to 800 Hz for the stacked PMMA films consisting of 65-nm-thick layers. The curves given for T_α are evaluated using Eq. (3).

law:

$$T_\alpha(t_a) = T_\alpha^0 + \left(T_\alpha^\infty - T_\alpha^0\right)\left[1 - \exp\left(-\frac{t_a}{\tau}\right)\right], \quad (3)$$

where $T_\alpha^0 \equiv T_\alpha(0)$, $T_\alpha^\infty \equiv T_\alpha(\infty)$, and τ is the characteristic time of the change in T_α during the annealing process at 409 K. From Eq. (3), the following master equation can be obtained:

$$\tilde{T_\alpha}(t_a) = 1 - \exp(-\tilde{t_a}), \quad (4)$$

where $\tilde{T_\alpha}$ and $\tilde{t_a}$ are defined by

$$\tilde{t_a} \equiv \frac{t_a}{\tau}, \qquad \tilde{T_\alpha}(t_a) \equiv \frac{T_\alpha(t_a) - T_\alpha^0}{T_\alpha^\infty - T_\alpha^0}. \quad (5)$$

The curves in Fig. 4 are calculated using Eq. (3) and are very close to the observed values of T_α for a wide range of t_a values, except for the initial value at $t_a = 0$. After rescaling the observed values of T_α using the normalized $\tilde{t_a}$ and $\tilde{T_\alpha}$ defined by Eq. (5), the data for all frequencies between 20 and 310 Hz can well be reduced to a master curve given by Eq. (4), as shown in Fig. 5. This scaling behavior can be observed not only for stacked PMMA thin films consisting of 65-nm-thick layers, but also for those of 41- and 15-nm-thick layers. From

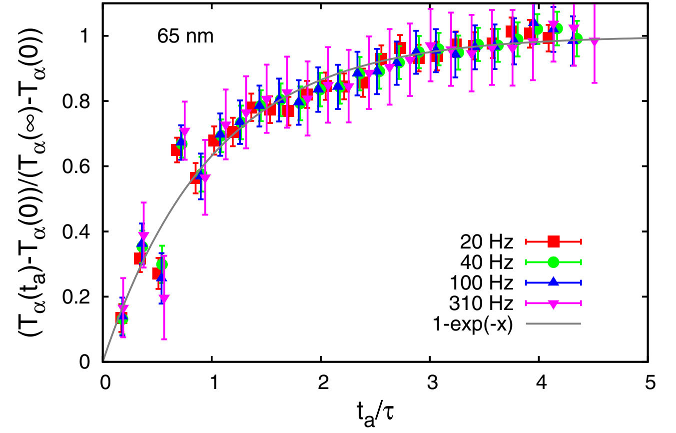

FIG. 5. (Color online) The dependence of the reduced α-peak temperature on the reduced annealing time $\tilde{t_a}$, at various frequencies for the stacked PMMA thin films consisting of 65-nm-thick layers, during the annealing process at 409 K. The curve is evaluated from Eq. (4).

fitting the observed values of T_α to Eq. (3), the characteristic time τ can be evaluated as a function of frequency. In Fig. 6 the value of τ for a change in T_α during the annealing process is a decreasing function of f.

These results suggest that there is a universal mechanism for the annealing effects on the α process over a large frequency range. Only the characteristic time τ changes with the frequency of the applied electric field and the annealing time. In this case, it can be concluded that the change in the dynamics of the α process occurs from the high-frequency side to the low-frequency one, i.e., small-scale motion changes earlier than large-scale motion does.

C. Widths of the dielectric loss peaks and relaxation strengths of the α and β processes

Figure 7 shows the annealing time dependence of the relative width in the temperature domain of the dielectric loss

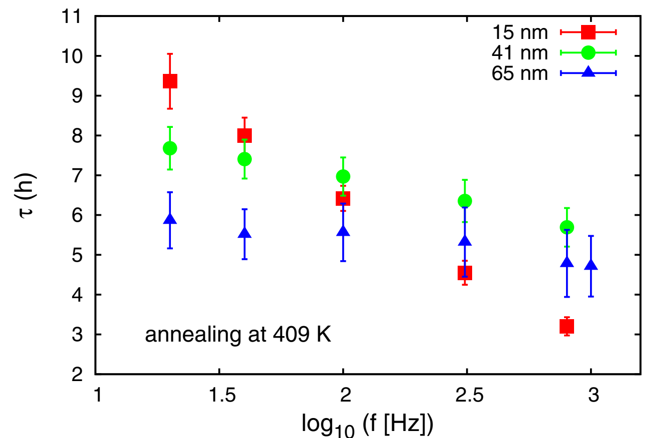

FIG. 6. (Color online) The frequency dependence of the characteristic time τ of the change in T_α during the annealing process for the stacked thin films consisting of PMMA layers of 15, 41, and 65 nm thickness.

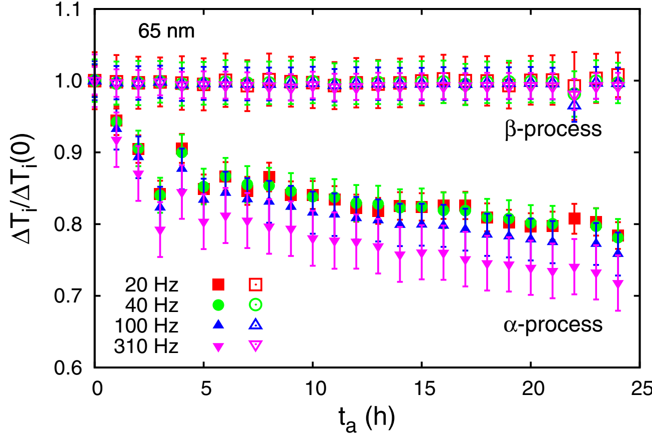

FIG. 7. (Color online) The annealing time dependence of the relative width of the loss peak due to the α and β processes for the stacked PMMA thin films consisting of 65-nm-thick layers. Filled symbols are for the α process and open ones are for the β process. The width in the temperature domain at the annealing time t_a for a given frequency is normalized with respect to the value at $t_a = 0$. The average values between ΔT_β^l and ΔT_β^r are used as the width for the β process.

peaks due to the α and β processes, for the stacked PMMA thin films consisting of 65-nm-thick layers, at various frequencies. The width is normalized with respect to the value at the initial time $t_a = 0$. This relative width in the temperature domain can be associated with the width of the distribution of relaxation times of the α process, τ_α (β process, τ_β) in the time domain and/or the variation in the local activation energy of the α process (β process). In Fig. 7 the width ΔT_β remains almost unchanged during the annealing process, while the relative width $\Delta T_\alpha/\Delta T_\alpha(0)$ decreases to about 0.7 with increasing annealing time t_a. In other words, neither the distribution of the relaxation times nor the local activation energy of the β process changes with t_a. However, this is not the case for the α process of stacked PMMA thin films during the annealing process. Although the reduction of the broadening of the dielectric loss peak of the α process for the annealing process was observed in the frequency domain at a given temperature for stacked PS thin films [24], it is difficult to judge whether there is the reduction in the broadening of the dielectric loss peak in the frequency domain for stacked PMMA thin films, because of the overlap of the α and β processes and the contributions from dc conductivity. Hence, it is assumed here that the variation in local activation energy of the α process is the origin of the reduction in the width ΔT_α during the annealing process. On this assumption, the observed narrowing of the width ΔT_α suggests that the local activation energy of the α process increases with increasing annealing time for the annealing process. This increase in local activation energy is strongly associated with a strong to fragile transition, as will be discussed later.

Figure 8 shows the annealing time t_a dependence of the relaxation strength of the α and β processes, $\Delta\varepsilon_\alpha$ and $\Delta\varepsilon_\beta$ for the stacked PMMA thin films consisting of 65-nm-thick layers, during the annealing process at 409 K for various frequencies from 20 to 800 Hz. The sum of the relaxation strength of the α and β processes, $\Delta\varepsilon_\alpha + \Delta\varepsilon_\beta$, is also shown in Fig. 8. The relaxation strength of the α process decreases with annealing time t_a, while that of the β process increases during the annealing process. However, the sum of the relaxation strengths of both the processes remains almost constant. Assuming that the orientational polarization of the dipole moment is the origin of the dielectric strength $\Delta\varepsilon$, and that the interaction between the orientational motions of the dipole moments can be neglected, the following relation is obtained: $\Delta\varepsilon = \frac{N\mu^2}{3k_BT}$, where N is the number density of the dipole moments associated with orientational motion, μ is the dipole moment of the motional unit, and k_B is the Boltzmann constant. Therefore, the present experimental result suggests that the number density of the dipole moments, which play a crucial role in the α process of as-stacked PMMA thin films, decreases with t_a, while the number density of the dipole moments associated with the β process increases at the expense of the number density of the dipoles associated with the α process. This means that there is a strong coupling between the microscopic origins of the α and β processes, although the temperatures T_α and T_β show no correlation with respect to the annealing time dependence. For bulk PMMA, the coupling between the α and β processes has been investigated by multidimensional NMR [40] and dielectric relaxation spectroscopy [41,42]. Spiess *et al.* showed that in PMMA, the β process predominantly influences the time scale of the α process, leading to particularly high mobility of the main chain itself. Grohens *et al.* showed the existence of a cooperative interaction between the side-chain and backbone motions in isotactic PMMA and to a lesser extent in syndiotactic PMMA using the ratio of intensities of infrared absorption peaks [43]. This coupling observed in bulk PMMA may be related to conversion from the α process to the β process.

For freely standing PMMA films, Roth *et al.* observed the reduction of T_g using transmission ellipsometry and showed that the magnitude of the T_g reductions for freely standing PMMA films is smaller than those for freely standing PS films [44]. They explained the observed difference of the maginitudes of T_g reductions between PMMA and PS using the following assumptions on the basis of the above coupling between the α and β processes. If there is this coupling, a certain fixed fraction of the total thermal energy present in the α and β processes manifests itself as motion associated with the β process at a given temperature, and there is also a continuous exchange of energy from the α process to the β process. In this case, the T_g of the PMMA thin films should decrease with decreasing film thickness less quickly than that of the PS thin films, because there is an energy transfer from the α process to the β process only for the PMMA thin films due to the coupling.

The present result in Fig. 8 can be interpreted as follows: the energy dissipated by the α process decreases with annealing time, while the one by the β process increases with annealing time. From our measurements in Ref. [24] and this paper, the magnitudes of T_g reduction from the bulk value, ΔT_g, are 26, 22, and 9 K for as-stacked PS, P2CS, and PMMA films consisting of 13-, 18-, and 15-nm-thick layers, respectively. Furthermore, the characteristic times, τ, for a change in T_α

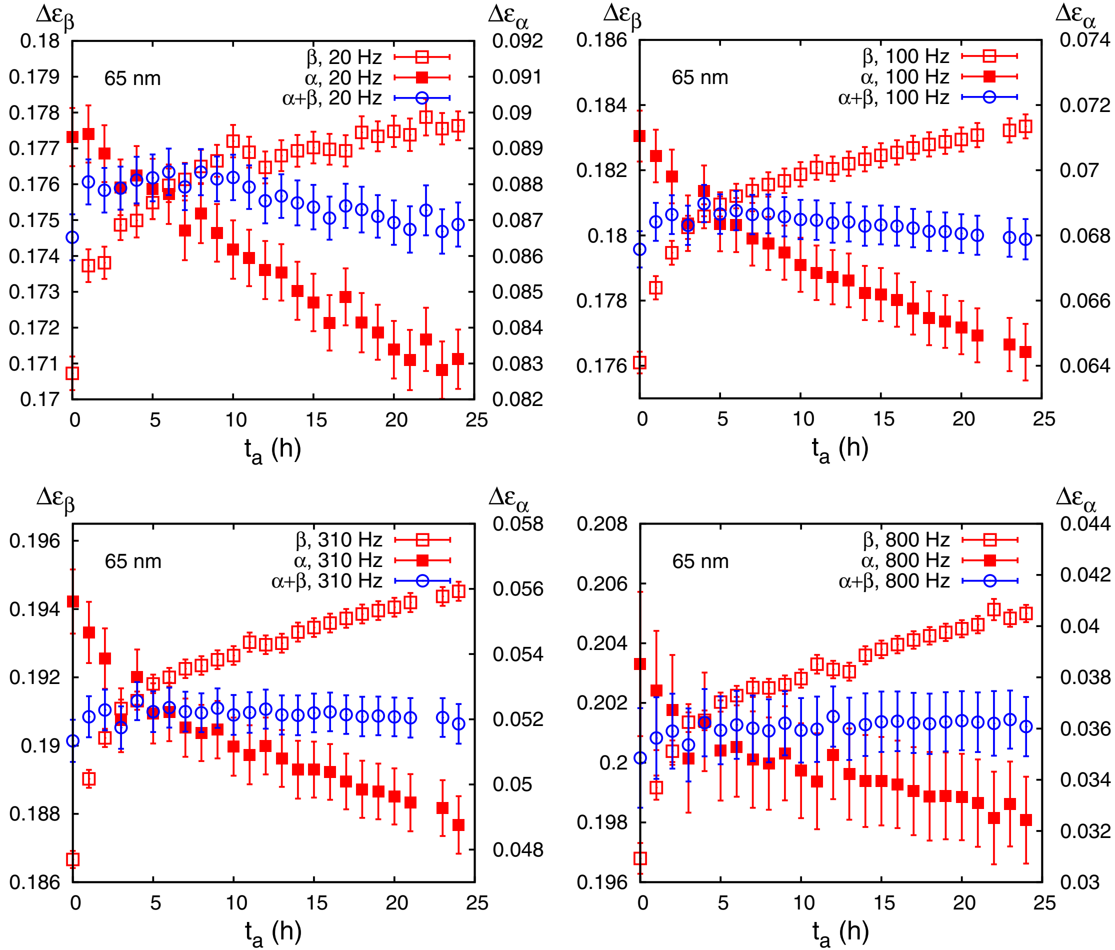

FIG. 8. (Color online) The annealing time t_a dependence of the relaxation strength of the α and β processes at various frequencies from 20 to 800 Hz for stacked PMMA thin films consisting of 65-nm-thick layers. The open and filled squares stand for the values of the β and α processes, respectively. The open circle stands for the sum of the relaxation strength of both the β and α processes. The values of the sum $\Delta\varepsilon_\alpha + \Delta\varepsilon_\beta$ are shifted along the vertical axis by an arbitrary amount for ease of comparison.

during annealing process at T_a are 29–45 h at $T_a = 425$–412 K for P2CS, while those are 6–9 h at $T_a = 409$ K for PMMA. Here it should be noted that the M_w of PS, P2CS, and PMMA used in the measurements are 2.8×10^5, 3.3×10^5, and 5.4×10^5, respectively. This suggests that the T_α can increase more quickly for the stacked PMMA thin films than for the stacked P2CS thin films. These experimental results can be well explained by the idea proposed by Roth *et al.* [44]. Furthermore, it can be expected that the ΔT_g and τ for stacked thin films of isotactic PMMA should be smaller than those of atactic PMMA, because the coupling between the α and β processes is stronger for isotactic PMMA than for atactic PMMA [43]. Therefore, the dependence of the dynamics of the stacked PMMA thin films on tacticity will be highly desired to check the validity of the above interpretation.

In this section, the majority of the experimental results discussed are for stacked PMMA thin films consisting of 65-nm-thick layers, as these serve as an example. For stacked PMMA thin films consisting of 41- and/or 15-nm-thick layers, it should be noted that near similar results are observed, and thus the above results are common amongst stacked thin films of PMMA layers of three different thicknesses.

D. Dynamics of stacked PMMA thin films

In Secs. IV A–IV C, the dielectric relaxation behavior of stacked PMMA thin films was discussed on the basis of the results observed in the temperature domain. Here further dielectric results are shown for more insightful discussion. Figure 9 shows dispersion maps of stacked PMMA thin films consisting of 15-nm-thick layers. The temperature dependence of the relaxation rate of the β and α processes is shown in Figs. 9(a) and 9(b), respectively. Here the α- and β-peak temperatures T_α and T_β are evaluated from the temperature dispersion of the dielectric loss spectra at a given frequency f, so that the data set (T_α, f) and (T_β, f) are obtained. These data sets are plotted as the data sets (T, f_α) and (T, f_β) in Figs. 9(b) and 9(a), respectively.

As shown in Fig. 9(a), the relaxation rates of the β process for various annealing times t_a from 0 to 24 h are sufficiently reduced to a single straight line. This suggests that the dynamics of the β process of stacked PMMA thin films remain unchanged during the annealing process at 409 K. From the slope of the straight line in Fig. 9(a), we can conclude that the microscopic origin of the β process is controlled by a thermally activated process with an activation

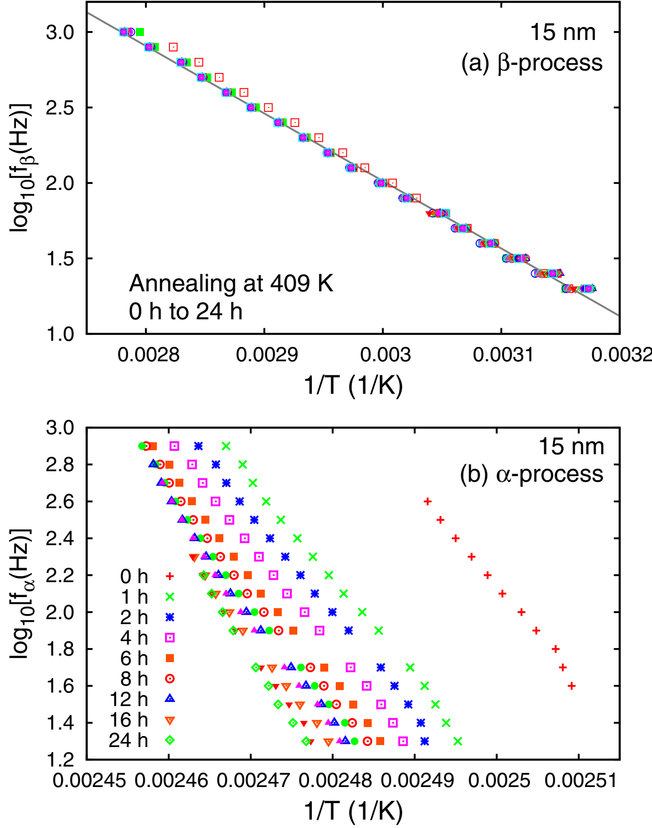

FIG. 9. (Color online) Dispersion map of α and β processes at various annealing times from 0 to 24 h for the stacked PMMA thin films consisting of 15-nm-thick layers during the annealing process at 409 K. (a) β process and (b) α process. The straight line is given by the Arrhenius law with an activation energy of 20.42 ± 0.05 kcal/mol.

energy of 20.42 ± 0.05 kcal/mol. This value agrees well with that reported in the literature [32]. Contrary to the β process, Fig. 9(b) shows that the temperature dependence of the relaxation rate of the α process, f_α, changes significantly with increasing annealing time t_a during the annealing process. At a given temperature, f_α decreases with increasing annealing time, which suggests that the dynamics of the α process become slower with annealing.

In order to discuss in greater detail the temperature dependence of f_α for stacked PMMA thin films, the results obtained by DSC are combined with the results obtained by DRS. The data set (T_g, f_g) obtained by DSC is plotted in the dispersion map, as shown in Fig. 10. Here f_g is the relaxation rate of the α process at T_g, and is defined by $f_g = 1/2\pi\tau_g$, where $\tau_g = 10^3$ s. The DSC results for stacked thin films of PMMA layers with three different thicknesses were obtained in Sec. III. Here the data sets (T_g, f_g) obtained by DSC for as-stacked thin films consisting of PMMA layers of 80, 48, and 15 nm thickness are coupled with the data sets (T_α, f) observed at $t_a = 0$ h for stacked thin films of PMMA layers of 65, 41, and 15 nm thickness, respectively. Furthermore, the data set (T_g, f_g) obtained by DSC for the bulk PMMA is coupled with all the data observed at $t_a = 24$ h during the annealing process for stacked thin films of PMMA layers of three different thicknesses.

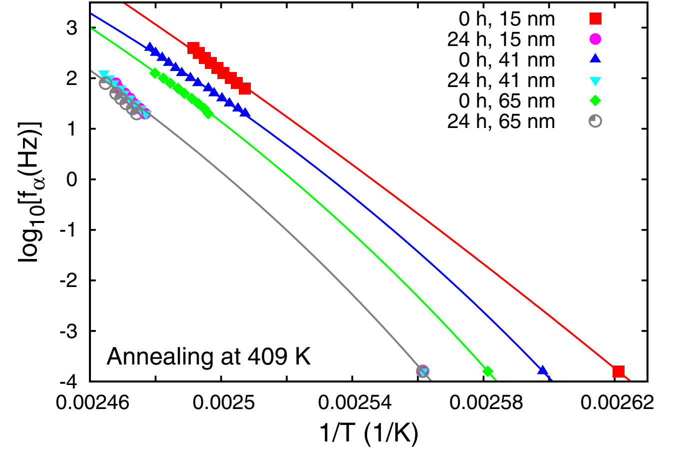

FIG. 10. (Color online) Dispersion map of the α process at $t_a = 0$ and 24 h during the annealing process at 409 K, for stacked thin films of PMMA layers with various film thicknesses. The curves are evaluated using Eq. (6) with the best fitting parameters listed in Table III.

Figure 10 shows the temperature dependence of the relaxation rate of the α process before and after the annealing at 409 K, for the stacked thin films of PMMA layers of various film thicknesses. In Fig. 10 the relaxation rate of the α process has a stronger temperature dependence than that of the β process, which is given by the Arrhenius law. The temperature dependence changes with the thickness of a single layer in the as-stacked PMMA thin films and also changes with annealing. In order to evaluate this temperature dependence of the relaxation rate of the α process, the Vogel-Fulcher-Tammann (VFT) law is adopted [45–48]:

$$\tau_\alpha(T) = \tau_{\alpha,0} \exp\left(\frac{U}{T - T_V}\right), \tag{6}$$

where τ_α is given by the relation $\tau_\alpha = 1/2\pi f_\alpha$, $\tau_{\alpha,0}$ is a positive constant, U is the apparent activation energy, and T_V is the Vogel temperature. The best-fitting parameters of VFT law are listed in Table III. Using the values of U, T_V, and T_g, the fragility index m is also evaluated by the following definition [49]:

$$m = \left[\frac{d \log_{10} \tau_\alpha(T)}{d(T_g/T)}\right]_{T=T_g}. \tag{7}$$

As shown in Fig. 10, the temperature dependence of the relaxation rate of the α process can be well reproduced by the VFT law. Furthermore, Table III shows that the Vogel

TABLE III. The thickness of the single layer d, the glass transition temperature T_g, the Vogel temperature T_V, the apparent activation energy U, and the fragility index m.

d (nm)	T_g (K)	T_V (K)	U (K)	m
Bulk	390.4	341.0	2756	191.5
65, 80	387.4	335.1	3068	188.4
41, 48	384.9	329.4	3236	175.4
15, 15	381.5	237.9	17283	138.8

temperature T_V increases from 238 to 341 K as the thickness of the single layer in the as-stacked PMMA thin films increases from 15 nm to the bulk. Accordingly, the fragility index m increases from 139 to 192. This suggests that the temperature dependence of τ_α changes from an Arrhenius-like one to a VFT one. In other words, the glassy dynamics of the as-stacked thin films change from strong to fragile, as the thickness of each single layer increases. The existence of the transition from strong to fragile can be also supported by the reduction in the peak broadening of the dielectric loss with annealing, as discussed in Sec. IV C. This thickness dependence of the α process of stacked PMMA thin films is consistent with that of stacked P2CS thin films [24] and is also consistent with that observed for single thin films of PS [50]. Therefore, it can be concluded that the fragile to strong transition, which is observed by confinement [51–56], is present for stacked thin films of PMMA and P2CS, as the thickness of each single layer decreases from the bulk to a few nm in thickness.

V. CONCLUDING REMARKS

In this study, the T_g and the dynamics of the α and β processes have been investigated using DSC and DRS for stacked PMMA thin films during the annealing process. The results can be summarized as follows:

(1) The T_g and the dynamics of the α process of as-stacked PMMA thin films exhibit thin-film-like behavior, in that the glass transition temperature is depressed and the dynamics of the α process are faster than those of the bulk system.

(2) Annealing at high temperatures causes T_g and the relaxation time of the α process to increase to those of the bulk. The fragility index of as-stacked PMMA thin films increases from 138 to 192 with increasing thickness of the single layer from 15 nm to the bulk value.

(3) The relaxation time of the β process of stacked PMMA thin films is almost equal to that of the bulk PMMA and is unaffected by annealing.

(4) The relaxation strengths of the α and β processes show a strong correlation between them and the sum of the relaxation strengths remains almost unchanged, while the individual relaxation strengths change during annealing process.

The results obtained by DSC clearly showed that the T_g of as-stacked PMMA thin films is depressed from the bulk T_g and is returned to the bulk T_g after annealing at high temperatures. This strongly suggests the existence of mobile interfacial regions between two PMMA thin layers. Hence, a thin PMMA layer in stacked PMMA films can be regarded as an ideal thin polymer film covered with mobile regions on both sides, and this might be similar to freely standing thin films.

In our previous study [57], both T_α and T_β for PMMA single thin films supported on an Al-deposited glass substrate, and covered with an upper Al layer, decrease with decreasing film thickness. These results are different from the results of the present measurements for stacked PMMA thin films. In the case of stacked PMMA thin films, most of the thin PMMA layers are covered with other thin layers of the same polymer on both sides, and only the thin PMMA layers located on the top or bottom of the stack are covered with a thin gold layer on one side. Thus, the difference between the previous and present results should come from the difference in interactions between the substrate and polymer. As shown in Ref. [39], the T_g of PMMA thin films strongly depends on the substrate material, and hence we can say that the T_g of the PMMA thin films is very sensitive to interactions between the substrate and polymer. As the thin layers in stacked PMMA thin films can be an ideal system, as mentioned earlier in this paper, we believe that the present thickness dependence of T_α and T_β is intrinsic to the nature of the dynamics of PMMA thin films.

Our experimental results clearly show that there is a strong correlation between the depression of T_g and the decrease in fragility index. This suggests that the fragility can play a crucial role in determining the glass transition temperature and the related dynamics in thin polymer films. Recently Evans *et al*. reported that there is a strong correlation between the fragility index and the depression of T_g in thin polymer films on the basis of fluorescence measurements of polymeric systems with various fragility indices [58].

In this study the observed experimental results suggest that the interfacial interaction can play a crucial role in determining the depression of T_g and the speed-up of the dynamics of the α process, while leaving unaffected the properties of the β process, except for its dielectric relaxation strength. Furthermore, there should be a possibility of controlling the glass transition dynamics of thin polymer films using an appropriate annealing condition. In order to understand the intricacies of the relationship between the interface and the dynamics of thin polymer layers, a direct investigation of the structure of the interface and the effect of annealing should be studied using x-ray or neutron reflectivity measurements, as the next step in this study.

ACKNOWLEDGMENTS

This work was supported by a Grant-in-Aid for Scientific Research (B) (No. 25287108) and Exploratory Research (No. 25610127, No. 23654154) from the Japan Society for the Promotion of Science. One of the authors (K.F.) would like to express his cordial thanks to Dr. Didier Long for giving him an opportunity to stay in his laboratory in Lyon as a visiting professor of CNRS, where most of the present paper has been written. The authors also thank the anonymous reviewers for giving them valuable suggestions that improved the content of the original manuscript.

[1] K. L. Ngai, in *Physical Properties of Polymers*, edited by J. Mark (Cambridge University Press, Cambridge, 2004), pp. 72–152.

[2] H. Sillescu, J. Non-Cryst. Solids **243**, 81 (1999).

[3] L. Berthier, G. Biroli, J.-P. Bouchaud, L. Cipelletti, and W. van Saarloos, *Dynamical Heterogeneities in Glasses, Colloids, and Granular Media* (Oxford University Press, New York, 2011).

[4] T. Muranaka and Y. Hiwatari, Phys. Rev. E **51**, R2735 (1995).

[5] R. Yamamoto and A. Onuki, Phys. Rev. E **58**, 3515 (1998).
[6] E. R. Weeks, J. C. Crocker, A. C. Levitt, A. Schofield, and D. A. Weitz, Science **287**, 627 (2000).
[7] G. Adam and J. H. Gibbs, J. Chem. Phys. **43**, 139 (1965).
[8] M. Alcoutlabi and G. B. McKenna, J. Phys.: Condens. Matter **17**, R461 (2005).
[9] S. Napolitano, S. Capponi, and B. Vanroy, Eur. Phys. J. E **36**, 61 (2013).
[10] M. Y. Efremov, A. V. Kiyanova, J. Last, S. S. Soofi, C. Thode, and P. F. Nealey, Phys. Rev. E **86**, 021501 (2012).
[11] M. Tress, M. Erber, E. U. Mapesa, H. Huth, J. Müller, A. Serghei, C. Schick, K.-J. Eichhorn, B. Voit, and F. Kremer, Macromolecules **43**, 9937 (2010).
[12] Z. Fakhraai and J. A. Forrest, Science **319**, 600 (2008).
[13] Z. Yang, Y. Fujii, F. K. Lee, C.-H. Lam, and O. K. C. Tsui, Science **328**, 1676 (2010).
[14] A. D. Schwab, D. M. G. Agra, J.-H. Kim, S. Kumar, and A. Dhinojwala, Macromolecules **33**, 4903 (2000).
[15] K. Tanaka, K. Hashimoto, T. Kajiyama, and A. Takahara, Langmuir **19**, 6573 (2003).
[16] D. Kawaguchi, K. Tanaka, T. Kajiyama, A. Takahara, and S. Tasaki, Macromolecules **36**, 1235 (2003).
[17] T. Kajiyama, K. Tanaka, and A. Takahara, Macromolecules **30**, 280 (1997).
[18] S. F. Swallen, K. Traynor, R. J. McMahon, M. D. Ediger, and T. E. Mates, Phys. Rev. Lett. **102**, 065503 (2009).
[19] S. F. Swallen, K. Windsor, R. J. McMahon, M. D. Ediger, and T. E. Mates, J. Phys. Chem. B **114**, 2635 (2010).
[20] S. Capponi, S. Napolitano, and M. Wübbenhorst, Nat. Commun. **3**, 1233 (2012).
[21] Y. P. Koh, G. B. McKenna, and S. L. Simon, J. Polym. Sci. Part B: Polym. Phys. **44**, 3518 (2006).
[22] Y. P. Koh and S. L. Simon, J. Polym. Sci. B **46**, 2741 (2008).
[23] K. Fukao, Y. Oda, K. Nakamura, and D. Tahara, Eur. Phys. J. Special Topics **189**, 165 (2010).
[24] K. Fukao, T. Terasawa, Y. Oda, K. Nakamura, and D. Tahara, Phys. Rev. E **84**, 041808 (2011).
[25] K. Fukao, T. Terasawa, K. Nakamura, and D. Tahara, in *Glass Transition, Dynamics and Heterogeneity of Polymer Thin Films*, edited by T. Kanaya (Springer, Berlin, 2013), Vol. 252 of Advances in Polymer Science, pp. 65–106.
[26] J. L. Keddie, R. A. L. Jones, and R. A. Cory, Europhys. Lett. **27**, 59 (1994).
[27] K. Fukao and Y. Miyamoto, Phys. Rev. E **61**, 1743 (2000).
[28] R. D. Priestley, L. J. Broadbelt, J. M. Torkelson, and K. Fukao, Phys. Rev. E **75**, 061806 (2007).
[29] K. Schmidt-Rohr, A. S. Kulik, H. W. Beckham, A. Ohlemacher, U. Pawelzik, C. Boeffel, and H. W. Spiess, Macromolecules **27**, 4733 (1994).
[30] G. Fytas, C. H. Wang, E. W. Fischer, and K. Mehler, J. Polym. Sci. Part B: Polym. Phys. **24**, 1859 (1986).
[31] H. Sasabe and S. Saito, J. Polym. Sci. Part A-2: Polym. Phys. **6**, 1401 (1968).
[32] N. G. McCrum, B. E. Read, and G. Williams, *Anelastic and Dielectric Effects in Polymeric Solids* (John Wiley, London, 1967).
[33] M. Ardi, W. Dick, and J. Kubát, Colloid Polym. Sci. **271**, 739 (1993).
[34] J. L. G. Ribelles and R. D. Calleja, J. Polym. Sci.: Polym. Phys. Ed. **23**, 1297 (1985).
[35] R. Bergman, F. Alvarez, A. Alegría, and J. Colmenero, J. Chem. Phys. **109**, 7546 (1998).
[36] K. Paeng and M. D. Ediger, Macromolecules **44**, 7034 (2011).
[37] K. Paeng, R. Richert, and M. D. Ediger, Soft Matter **8**, 819 (2012).
[38] K. Fukao and Y. Miyamoto, Europhys. Lett. **46**, 649 (1999).
[39] J. L. Keddie, R. A. L. Jones, and R. A. Cory, Faraday Discuss. **98**, 219 (1994).
[40] S. C. Kuebler, D. J. Schaefer, C. Boeffel, U. Pawelzik, and H. W. Spiess, Macromolecules **30**, 6597 (1997).
[41] J. Ménégotto, P. Demont, and C. Lacabanne, Polymer **42**, 4375 (2001).
[42] S. Doulut, C. Bacharan, P. Demont, A. Bernès, and C. Lacabanne, J. Non-Cryst. Solids **235–237**, 645 (1998).
[43] Y. Grohens, R. E. Prud'homme, and J. Schultz, Macromolecules **31**, 2545 (1998).
[44] C. Roth, A. Pound, S. Kamp, C. Murray, and J. Dutcher, Eur. Phys. J. E **20**, 441 (2006).
[45] H. Vogel, Phys. Z. **22**, 645 (1921).
[46] G. S. Fulcher, J. Am. Ceram. Soc. **8**, 339 (1925).
[47] G. S. Fulcher, J. Am. Ceram. Soc. **8**, 789 (1925).
[48] G. Tammann and W. Hesse, Z. Anorg. Allg. Chem. **156**, 245 (1926).
[49] R. Böhmer and C. A. Angell, Phys. Rev. B **45**, 10091 (1992).
[50] K. Fukao and Y. Miyamoto, Phys. Rev. E **64**, 011803 (2001).
[51] C. Zhang, Y. Guo, K. B. Shepard, and R. D. Priestley, J. Phys. Chem. Lett. **4**, 431 (2013).
[52] S. Napolitano and M. Wübbenhorst, Polymer **51**, 5309 (2010).
[53] H. Yin, S. Napolitano, and A. Schönhals, Macromolecules **45**, 1652 (2012).
[54] A. Huwe, F. Kremer, P. Behrens, and W. Schwieger, Phys. Rev. Lett. **82**, 2338 (1999).
[55] R. A. Riggleman, K. Yoshimoto, J. F. Douglas, and J. J. de Pablo, Phys. Rev. Lett. **97**, 045502 (2006).
[56] T. S. Jain and J. J. de Pablo, J. Chem. Phys. **120**, 9371 (2004).
[57] K. Fukao, S. Uno, Y. Miyamoto, A. Hoshino, and H. Miyaji, Phys. Rev. E **64**, 051807 (2001).
[58] C. M. Evans, H. Deng, W. F. Jager, and J. M. Torkelson, Macromolecules **46**, 6091 (2013).